Carcinogenesis vol.26 no.7 pp.1224–1232, 2005
doi:10.1093/carcin/bgi066
Advance Access publication March 10, 2005

Effect of common *B-RAF* and *N-RAS* mutations on global gene expression in melanoma cell lines

Sandra Bloethner[1], Bowang Chen[1], Kari Hemminki[1,2], Jan Müller-Berghaus[3], Selma Ugurel[3], Dirk Schadendorf[3] and Rajiv Kumar[1,2,*]

[1]Division of Molecular Genetic Epidemiology, German Cancer Research Center, Im Neuenheimer Feld 580, 69120 Heidelberg, Germany, [2]Department of Biosciences, Karolinska Institute, 141 57 Huddinge, Sweden and [3]Skin Cancer Unit, German Cancer Research Center, Im Neuenheimer Feld 280, 69120 Heidelberg, Germany

[*]To whom correspondence should be addressed. Tel: +49 6221 42 1806; Fax: +49 6221 42 1810;
Email: r.kumar@dkfz.de

We studied global gene expression in three melanoma cell lines with the most common and potent V600E mutation in the *B-RAF* gene—four cell lines with a common Q61R mutation in the *N-RAS* gene and three cell lines with no mutations using human HG-U133A 2.0 micro-arrays with 22 277 transcripts. Data analysis using stringent criteria revealed several upregulated and downregulated genes in cell lines with *B-RAF* and *N-RAS* mutations compared with cell lines without mutations. We found 29 genes specifically upregulated and 32 genes downregulated in cell lines with *B-RAF* mutations, whereas 70 genes were upregulated and 39 downregulated in cell lines with *N-RAS* mutations; 11 genes showed overlapping upregulation and 45 downregulation. The micro-array data for nine selected genes were validated by the real-time PCR technique. Expression of a large number of genes, that encode members or regulators of the RAS/RAF/MEK/ERK pathways or are involved in metastasis or invasion, was affected in cell lines with mutations in *B-RAF* and *N-RAS*. Upregulated genes in cell lines with mutations included dual-specificity phosphatase 6 (*DUSP6*), sprouty 2 (*SPRY2*), v-akt murine thymoma viral oncogene homolog 3 (*AKT3*) and matrix metalloproteinase 14 (*MMP14*); downregulated genes included interleukin 18 (*IL18*), Krüppel-like factor 5 (*KLF5*) and inhibitor of DNA binding 2 (*ID2*). Our results, though carried on cell lines, provide a novel insight into the effect of mutations in the *B-RAF* and *N-RAS* genes on global gene expression in melanoma and highlight the complexity of mechanisms involved in tumour initiation and maintenance.

Introduction

The Ras/Raf/MEK/ERK signalling pathway has been shown to be constitutively activated in melanoma either due to oncogenic mutations in the *B-RAF* or *N-RAS* genes or through autocrine growth factor stimulation (1,2). In melanocytes ERK is also activated in cAMP-dependent signalling cascade as a consequence of α-melanocyte-stimulating hormone and related peptide binding to melanocortin receptor 1 with *B-RAF* as a key intermediate (3,4). The importance of *B-RAF* is emphasized by occurrence of mutations in the gene at a high frequency in melanomas and benign melanocytic nevi (5–9). Mutations in the *B-RAF* gene mainly affect the kinase activation domain, most, but not all, of which are associated with an increased kinase activity (10).

The V600E mutant, accounting for over 90 percent of all *B-RAF* mutations detected in melanoma and melanocytic nevi, obviates the requirement for activation segment phosphorylation of the T599 and S602 residues that occurs during the normal activation of the kinase (5,8,9). This mutant, in *in vitro* experiments, is associated with an over 400-fold greater basal activity and it induces focus formation in NIH3T3 cells with a much higher efficiency than the wild-type *B-RAF* (5,10). The functional relevance of the V600E *B-RAF* mutant has also been shown by its induction of MEK and ERK in melanocytes, tumorigenicity in nude mice and evidence of spontaneous immune response in melanoma patients with mutation (11,12). Depletion of the mutant *B-RAF* by siRNA has been shown to block MEK–ERK signalling, cell cycle progression and abrogate transformation (13). Recently it has been reported that mutant *B-RAF* not only promotes cell proliferation but may also induce dedifferentiation (14).

Besides *B-RAF* mutations, melanomas to a lesser extent harbour oncogenic mutations in the *N-RAS* gene that are reported mainly to occur in lesions from sun-exposed sites. Activating mutations in the *N-RAS* gene not only result in the reduction of intrinsic GTPase activity but also in the induction of resistance against molecules inducing such activity. Mutations in the *N-RAS* mostly affect codon 61, one of the most common activating changes being glutamine to arginine substitution (15). Both functional and genetic evidence indicate that *B-RAF* and *N-RAS* act linearly in the signalling pathway, which is evidenced by almost mutual exclusiveness of mutations in these genes and consequent ERK activation (1,2,5).

Though a discernible picture of the effects of *B-RAF* and *N-RAS* mutants in melanoma cell lines has begun to emerge, the consequences of these mutants on global gene expression remain to be understood. A recent study based on cDNA micro-array has identified differences in expression between cell lines with and without *B-RAF* and *N-RAS* mutations (16). In the present study, using the Affymetix expression set up, we have focused on relative change in global gene expression in melanoma cell lines with most common and potent *BRAF* mutation V600E. In addition, we also included cell lines with *N-RAS* activating mutation (Q61R) and compared them with the expression profiles of cell lines with *B-RAF* mutations and cell lines lacking mutations in the two genes using three different software modules. The results from micro-array analysis for the most relevant transcripts, especially those encoding molecules involved in RAS/RAF/MEK/ERK signalling pathways, were validated by quantitative real time PCR.

Abbreviations: DUSP6, dual-specificity phosphatase 6; FDR, false discovery rate.

Materials and methods

Cell lines and cell culture

A panel of 117 melanoma cell lines derived from 88 individual patients were screened for mutations in the *B-RAF*, *N-RAS* and *CDKN2A* genes. Three cell lines Ma-Mel-16a, Ma-Mel-51 and Ma-Mel-57 with V600E mutation in the *B-RAF* gene; four cell lines UKRV-Mel-15d, UKRV-Mel-19a, Ma-Mel-28 and Ma-Mel-43 with Q61R mutation in the *N-RAS* gene; and three cell lines UKRV-Mel-4, UKRV-Mel-5 and UKRV-Mel-11 without mutations in the *B-RAF* and *N-RAS* genes were selected for expression experiments. Cell lines chosen for this investigation were established from tissue specimens of metastasized lesions from cutaneous melanoma. Ma-Mel-28, Ma-Mel-43, UKRV-Mel-5 were derived from cutaneous or subcutaneous lesions; Ma-Mel-51, Ma-Mel-57, UKRV-Mel-11, UKRV-Mel-15d and UKRV-Mel-19a from lymph node metastases: UKRV-Mel-4 was from liver metastasis and Ma-Mel-16a was from small bowel metastasis. All the cell lines included for expression experiments in this study were derived from tumours from separate individual patients and none carried mutations or homozygous deletions at the *CDKN2A* locus.

In order to establish the cell lines, the tumour specimens were minced and thereafter maintained in RPMI 1640 (Life Technologies, Grand Island, NY) supplemented with 10% fetal calf serum (Life Technologies), 5 mM L-glutamine, 100 U/ml penicillin and 100 μg/ml streptomycin at 37°C in a humidified 5% CO_2 atmosphere. Established cell lines were used for analysis no later than six to eight passages. For isolation of DNA/RNA, all cell lines were cultured until 70–80% confluence, gently detached by 0.05% ethylenediaminetetraacetic acid/phosphate-buffered saline, washed twice, re-suspended in 10% fetal calf serum/RPMI and frozen down in liquid nitrogen until further analysis.

Isolation of RNA/DNA

Genomic DNA and total RNA were isolated from 2×10^6 cells with commercially available DNA/RNA Purification Kits (Gentra Systems, Minneapolis, MN). Total RNA was subjected to a second cleanup by a silica-gel-based membrane using RNeasy Mini Kit (Qiagen, Hilden, Germany). Concentrations of DNA and RNA were measured by UV spectrophotometry and OD 260/280 nm ratios between 1.9 and 2.1 were obtained for all RNA samples. The integrity of total RNA isolated from cell lines was determined on Bioanalyzer 2100 System (Agilent Technologies, Palo Alto, CA) using 400 ng RNA from each cell line.

Sample preparation and hybridization

Two micrograms of total RNA from each cell line was converted into double-stranded cDNA using SuperScript Double-Stranded cDNA Synthesis Kit (Invitrogen, Carlsbad, CA). First strand synthesis was carried out, by incubating at 42°C for 1 h, in a 20-μl volume reaction mix containing 50 μM T7-oligo(dT) primer (Qiagen, Hilden, Germany), 1× first strand cDNA buffer, 0.1 M DTT, 10 mM dNTP mix, 200 U SuperScript II Reverse Transcriptase and DEPC-treated H_2O. Second strand synthesis was performed at 16°C for 2 h in a final volume of 150 μl by adding 1× second strand reaction buffer, 10 mM dNTP mix, 10 U *Escherichia coli* DNA ligase, 40 U *E.coli* DNA polymerase I, 2 U *E.coli* RNase H and DEPC-treated H_2O to the first strand synthesis reaction. Incubation was prolonged for 5 min after addition of 10 U of T4 DNA polymerase to the reaction mix. The double-stranded cDNA was cleaned up with GeneChip Sample Cleanup Module (Affymetrix, Sunnydale, CA).

Twelve microlitres of the purified cDNA were used for the synthesis of biotin-labeled cRNA using ENZO Labeling Kit (Enzo, Farmingdale, NY). *In vitro* transcription reaction in a total volume of 40 μl that contained 4 μl 10× HY reaction buffer, 4 μl 10× biotin-labelled ribonucleotides, 4 μl 10× DTT, 4 μl 10× RNase inhibitor mix, 2 μl 20× T7 RNA polymerase and de-ionized H_2O was incubated at 37°C for 16 h. Twenty micrograms cleaned-up biotin-labelled cRNA from each reaction was cut into 35–200 bp fragments in a 40-μl volume reaction containing 8 μl 5× fragmentation buffer (Affymetrix, Sunnydale, CA) and RNase-free H_2O at 94°C for 35 min. Five micrograms of fragmented cRNA from each cell line was hybridized on Affymetrix Test3 arrays in order to test the entire procedure. Only those cRNA samples that showed at least 27% present calls and 3′ to 5′ signal ratios of 0.9–1.5 for the housekeeping genes ß-actin and GAPDH on the test arrays were loaded on Human HG-U133A 2.0 micro-arrays (Affymetrix) with 22 277 sequences (the list of genes is available at www.affymetrix.com). Ten micrograms (0.05 μg/μl) of fragmented labelled cRNA was hybridized onto the array at 45°C for 16 h. A 200-μl hybridization cocktail included 50 pM control oligonucleotide B2, 1.5, 5, 25 and 100 pM, as eukaryotic hybridization controls, 0.1 mg/ml herring sperm DNA, 0.5 mg/ml acetylated BSA, 1× hybridization buffer and H_2O. After hybridization micro-arrays were washed (GeneChip Fluidics Station 400, Affymetrix) and scanned (GeneArray Scanner, Affymetrix) according to Affymetrix protocols.

Data analysis

Image analysis. Image analysis was performed with the Affymetrix GeneChip Operating Software (GCOS) to analyse the scanned images, to convert intensities to a numerical format and to obtain a detection call. This call indicated whether a transcript was reliably detected (Present) or not detected (Absent). A detection *P*-value, which is calculated using the One-Sided Wilcoxon's Signed Rank test, reflects the confidence of the detection call. Additionally, a signal value was calculated for each probe set on the array using the One-Step Tukey's Biweight Estimate, which assigns a relative measure of abundance to the transcript. Target intensities from each array were scaled to a value of 100. The statistical algorithms used are described in further detail in Affymetrix 2002 GeneChip Expression Analysis at http://www.affymetrix.com/Download/manuals/data_analysis_fundamentals_manual.pdf.

Pair-wise comparison. GCOS was used for pair-wise comparisons of expression profiles between cell lines with mutation in the *B-RAF* and *N-RAS* genes and cell lines without mutations, which were designated as baseline arrays. During comparison analysis, each probe set on the experimental array was compared with its counterpart on the baseline array and a change in *P*-value was calculated indicating the change call: 'increase', 'marginal increase', 'decrease', 'marginal decrease' or 'no change' in gene expression. A second algorithm was used to calculate a quantitative estimate of the gene expression change in the form of signal log ratio. A signal log ratio of 1 or −1 corresponded to an increase or decrease, respectively, in transcript level by 2-fold. Further analysis that included sorting of data and identification of overlaps between changed probes was done by using Data Mining Tool (DMT) Software (Affymetrix). Probe sets that were 'absent' in both baseline samples and experimental samples were excluded. Secondly, comparisons with a 'no change' call were removed. Gene expression data were sorted according to the relative change and fold change values, and for identification of differentially expressed genes and data interpretation probe sets with a fold change ≥ 2 were used.

Analysis of micro-array data using SAM. SAM (significance analysis of micro-arrays) identifies genes with statistically significant changes in expression by assimilating a set of gene-specific *t*-tests (17). For comparison of cell lines with *B-RAF* mutation and cell lines without the mutation we chose delta = 1.05 and $R = 2$ (2-fold change or more) to obtain a number of up- and down-regulated probes numerically comparable to the number of probes obtained from analysis using the two other data analysis softwares. The resulting dataset yielded an estimated false discovery rate (FDR) of 18.5%. Similarly, to compare *N-RAS* mutated cell lines with cell lines without mutation a delta value of 1.59 and $R = 2$ were chosen with 7.3% FDR.

Marker analysis. Marker analysis was performed using GeneCluster 2.0 (18) to identify genes correlated with particular class distinction, cell lines with mutation versus cells without the mutation. The default settings for the filtering procedure were used as follows: genes were excluded if they exhibited <3-fold (max/min) and 100 U (max/min) absolute variations across the dataset after a threshold of 20 U and a ceiling of 16 000 were applied. The threshold of 20 U was set to avoid missing any potentially informative marker genes. Normalization of the dataset was performed by standardizing each row (probe set) to mean = 0 and variance = 1. To compare neighbours in the marker analysis a class template was created. We chose 300 markers for each class for this analysis to obtain probe lists numerically similar to those obtained by DMT and SAM softwares for the purpose of comparison. We analysed cell lines with *B-RAF* mutation and those with *N-RAS* mutation separately and data from cell lines without mutations were used as a baseline. The gene ranking method 'Signal to noise' was selected, which identified the difference of means in each of the classes scaled by the sum of standard deviations. The 'Signal to noise' statistics assign a lower ranking score to genes that have higher variance in each class—more than those genes that have a high variance in one class and a low variance in another.

Identification of genes. For gene identification and annotation we applied our data to Netaffx Analysis Center (Affymetrix web page), which maps the Affymetrix probe identifiers to gene identities including links to Gene Ontology and Pathway Softwares.

Quantitative real-time PCR

To confirm the validity of the micro-array expression data, the mRNA levels of 9 unique transcripts showing significant up or downregulation in cell lines with mutations compared to the ones without mutations were assessed by quantitative real-time PCR. The selections were based on the potential roles of the genes in melanocyte biology, the MAPK pathway or cell cycle regulation. cDNA was synthesized using 1 μg of total RNA (from the same batch as used in micro-array experiments) from each cell line and First Strand cDNA Synthesis Kit (Fermentas Life Sciences, St Leon-Rot, Germany). A 20-μl volume reaction contained 1 μl of 0.5 μg/μl $oligo(dT)_{18}$ primer, 4 μl of 5× reaction buffer, 20 U RiboLock ribonuclease inhibitor, 2 μl of 10 mM dNTP

mix, 40 U M-MuLV reverse transcriptase and DEPC-treated H_2O. The reaction mix was incubated at 37°C for 60 min following heat inactivation at 70°C for 10 min. cDNA samples were frozen at −80°C in small single-use aliquots until used.

Real-time PCR was carried out on an ABI PRISM 7900 Sequence Detection System (Applied Biosystems, Foster City, CA) and results analysed using the integrated Sequence Detection System Software Version 2.1. Reverse transcription reaction equivalent to 10 ng RNA was used, in triplicate, to amplify each cDNA using gene-specific primers and probes. The real-time PCR was carried out in a final volume of 20 μl containing 9 μl of diluted cDNA sample, 10 μl 2× TaqMan Universal Master Mix with AmpErase UNG (uracil-*N*-glycosylase) and 1 μl of 20× TaqMan Gene Expression Assay (Applied Biosystems, Foster City, CA). Thermocycle programme was set at initial hold 95°C for 10 min, followed by 40 cycles (45 cycles for down-regulated genes) of denaturation at 95°C for 15 s, annealing at 60°C and extension at 60°C for 1 min. A control human RNA (Stratagene, La Jolla, CA) was used for generating standard curves for β-actin (internal standard) and target genes by plotting C_t-values versus template copy numbers. The copy number of each target gene was normalized to that of house keeping gene β-actin using standard curves. The expression of each candidate gene was calculated as the ratio of the expression of that gene in cell lines with *B-RAF* and *N-RAS* mutations to those in cell lines carrying no mutation.

Results

In a panel of 117 melanoma cell lines, we detected mutations in the *B-RAF* gene in 70 (60%) cell lines and mutually exclusive mutations in the *N-RAS* gene in 24 (20%) cell lines. From this panel we selected cell lines, on the basis of mutational status of the *B-RAF*, *N-RAS* and *CDKN2A* genes, for studying expression profile using Affymetrix oligonucleotide arrays with sequences complementary to 22 277 probe sets. The expression profile of 3 melanoma cell lines harbouring the V600E mutation in the *B-RAF* gene and 4 cell lines with the Q61R mutation in the *N-RAS* gene was analysed and compared with the expression profile of 3 melanoma cell lines without mutations in the *B-RAF* and *N-RAS* genes. None of the cell lines chosen for this study carried any genetic alterations in the *CDKN2A* gene. Three different softwares, DMT (Affymetrix), SAM and GeneCluster 2.0 were used to analyse the micro-array data.

Results from micro-array data using GCOS and DMT

Expression analysis using the GCOS module showed that an average of 51% (11 380 ± 397.4) of transcripts were scored as being present in the cell lines harbouring the *B-RAF* mutation, an average of 53.7% (11 958 ± 78.1) of transcripts were present in cells containing the *N-RAS* mutation and an average of 52.4% (11 679 ± 96.5) of transcripts were present in cell lines without these mutations. We performed pair-wise comparison of expression data from each cell line with and without mutations. Therefore, from comparison with 3 cell lines from 3 individual patients with *B-RAF* mutation and without *B-RAF* mutation we obtained 9 datasets. Similarly, for 4 cell lines (from 4 individual patients) with *N-RAS* mutation and 3 cell lines (from 3 individual patients) without mutation 12 datasets were obtained. For sorting of data in DMT we applied two criteria, (i) change of expression level of '2 fold or more' (which equals to SLR of at least 1 or −1, respectively) and (ii) 100% concordance in increase or decrease of expression in each single comparison.

Based on these criteria, 174 probe sets corresponding to 139 genes were found to be increased in cell lines with the *B-RAF* mutation and 211 probe sets (168 genes) were decreased when compared with cell lines without the mutations. Similarly, cell lines harbouring the *N-RAS* mutations showed a significant increase of 275 probe sets (203 genes) and a decrease of 208 probe sets (168 genes). The combination of data from cell lines with the *B-RAF* and *N-RAS* mutations showed an overlap of 86 probes (69 genes) upregulated in cell lines with these mutations as compared to cell lines without mutations. In comparison to cell lines without mutations 88 probes (70 genes) were increased specifically in *B-RAF* mutated cell lines and 189 probes (134 genes) were increased only in cell lines with *N-RAS* mutation. One hundred and twelve probe sets (89 genes) showed an overlapping downregulation in cell lines with *B-RAF* and *N-RAS* mutations compared to cell lines without mutations. Similarly, in comparison to cell lines without mutations 99 probes (79 genes) were scored as decreased exclusively in cell lines with mutant *B-RAF* and 96 probes (79 genes) were found as significantly decreased only in cell lines with the *N-RAS* mutation.

Results from micro-array data using SAM

Using SAM for data analysis with a delta value of 1.05 and $R = 2$ (2-fold change or more), as described in Materials and methods, 696 probes were called significant (169 positive corresponding to 146 genes, 527 negative corresponding to 467 genes) for cell lines carrying the *B-RAF* mutation when compared to cell lines without the mutation. This number of probes compared well with the 174 positively and 211 negatively changed probes identified by DMT. However, the dataset yielded an estimated FDR of 18.5%, which equals to an average of 129 falsely significant genes. Normalization of signal values from cell lines with *N-RAS* mutation and the 767 probes (307 positive corresponding to 243genes/460 negative corresponding to 396 genes) without mutation to SAM with a delta of 1.59 (including the criteria of '2-fold or more change'), were called significant with 7.3% FDR corresponding to 56 genes.

Data from marker analysis using GeneCluster 2.0

For analysis of the micro-array data using GeneCluster 2.0, we used filter criteria as described in Materials and methods. For the cell lines with mutant *B-RAF*, 4546 probes passed these filters and for cell lines with the *N-RAS* mutation 4279 probes passed these criteria. For the purpose of further comparisons of the probe lists and the identification of overlapping probe sets between cell lines with mutations we chose the first 300 increased/decreased probe sets. Figure 1 shows a set of 20 best correlated markers which are distinct for each group of cell lines, whereas, Figure 2 displays a set of 30 best correlated markers that distinguish cell lines with either *B-RAF* or *N-RAS* mutations and cell lines without any mutations.

Combination of the data obtained from the three software modules

In order to increase the stringency of data analysis, we combined the list of genes obtained from the 3 software modules (Figure 3, Supplementary Tables I and II). In cell lines with the *B-RAF* mutation 40 genes were found to be significantly upregulated (Figure 3A) and 77 genes were significantly downregulated (Figure 3B) when compared with the cell lines containing no such mutations. Similar comparison showed that in cell lines with the *N-RAS* mutation 81 genes were with significantly increased expression (Figure 3C) and 84 genes with decreased expression (Figure 3D). We found that expression of 11 genes was significantly increased in cell lines with *B-RAF* and *N-RAS* mutations relative to cell lines without mutations (Figure 3E). Seventy genes appeared to

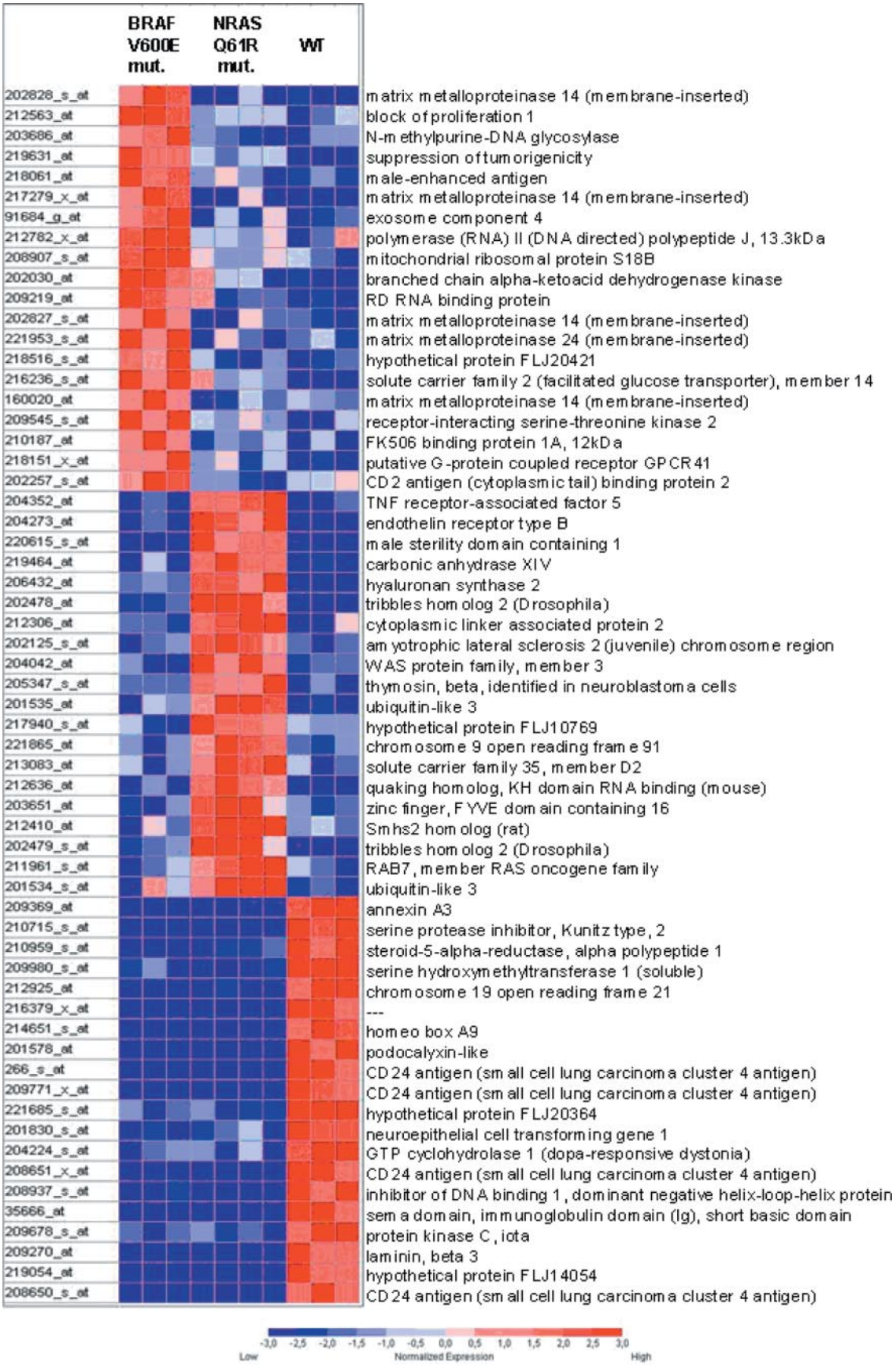

Fig. 1. Results from a marker gene analysis showed 20 best correlated genes with differential expressions in cell lines with *B-RAF* mutation, *N-RAS* mutation and cell lines without mutations. Markers were selected by computing the signal to noise score. The columns shown represent individual samples and rows represent single genes and are ranked in a 'best-correlated' order. The colour scale identifies relative gene expression changes normalized by the standard deviation, with 0 representing the mean expression level of a given gene across the panel.

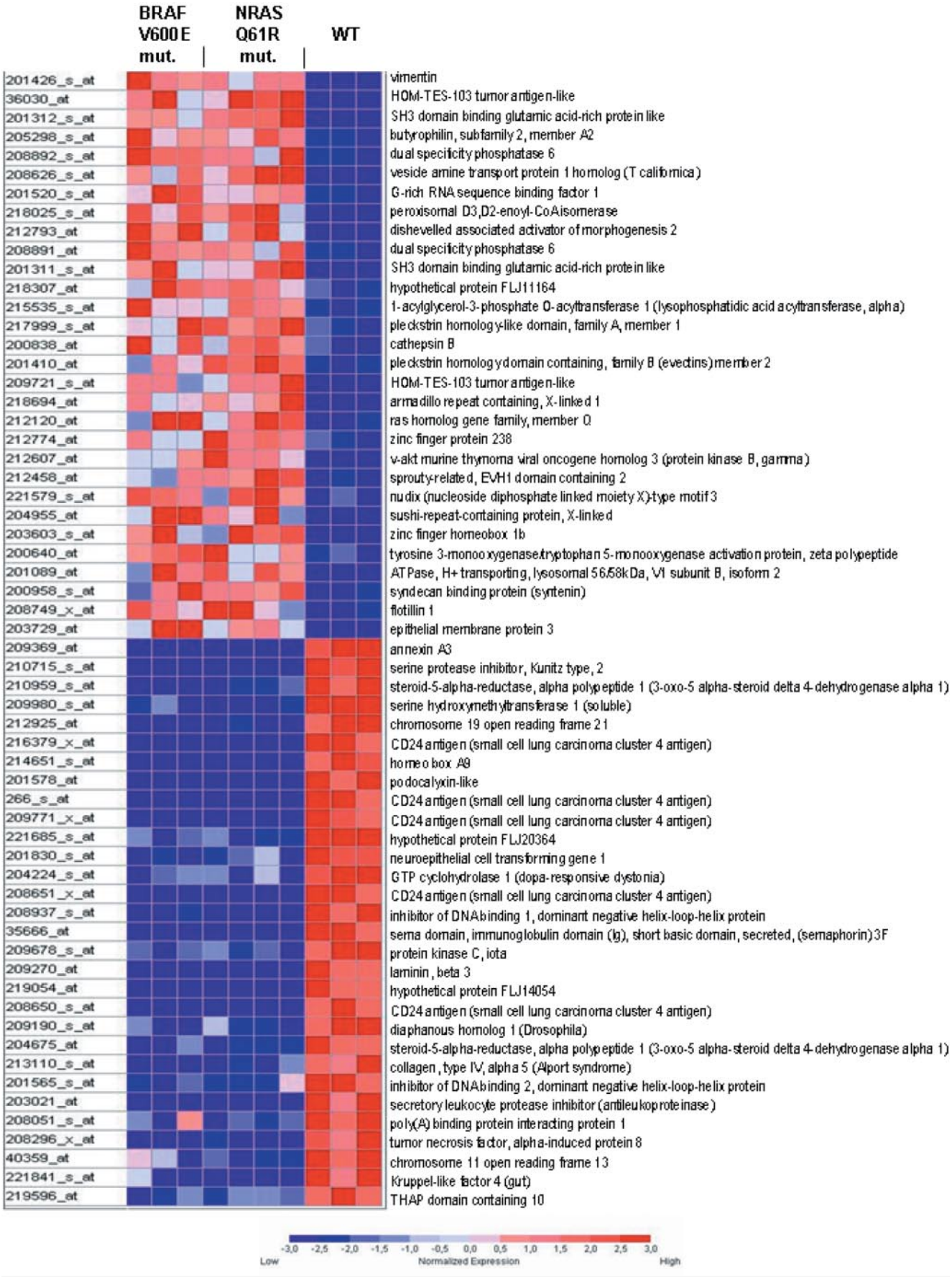

Fig. 2. Results from a marker gene analysis of micro-array data with 30 best correlated genes in cell lines with *B-RAF* and *N-RAS* mutations compared to cell lines with no mutations.

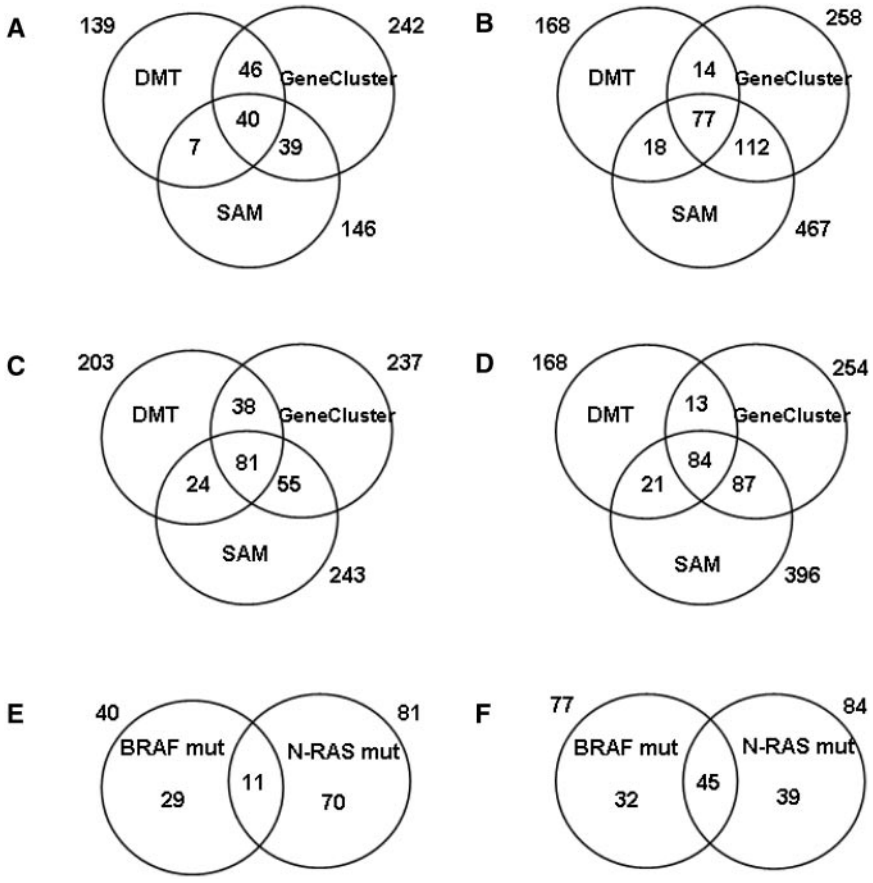

Fig. 3. Venn diagram representing the number of genes that showed differential expression in melanoma cell lines with *B-RAF* and *N-RAS* mutations compared to cell lines without mutations after evaluation of micro-array data with three different softwares (see Materials and methods). (**A**) Number of up-regulated genes in cell lines with *B-RAF* mutation against no mutations as shown by three different softwares; (**B**) down-regulated genes in cell lines with *B-RAF* mutation; (**C**) relative increased expression of genes in cell lines with *N-RAS* mutation; (**D**) decreased expression of genes in cell lines with *N-RAS* mutation; (**E**) filtered data from A–D showing number of common and specific genes upregulated in cell lines with *B-RAF* and *N-RAS* mutations; and (**F**) down-regulation of specific and common genes in cell lines with *B-RAF* and *N-RAS* mutations. See online supplementary material for a colour version of this figure.

be upregulated specifically in cell lines with the *N-RAS* mutation, 29 genes were markedly upregulated only in cell lines with the *B-RAF* mutation (Figure 3E and Supplementary Table I). Similarly 45 genes were downregulated in cell lines with the *B-RAF* and *N-RAS* mutations, 32 genes were specific to cell lines with the *B-RAF* mutations and 39 specific to cell lines with *N-RAS* mutations (Figure 3F and Supplementary Table II).

Some of the genes which showed a distinctive over-expression in cell lines with mutations in *B-RAF* and *N-RAS* genes in comparison to the cell lines without mutations included dual-specificity phosphatase 6 (*DUSP6*), v-akt murine thymoma viral oncogene homolog 3 (*AKT3*) and sprouty homolog 2 (*SPRY2*). In cell lines with mutations against cell lines without mutations interleukin 18 (*IL18*), tumor necrosis factor, alpha-induced protein 8 (*TNFAIP8*), inhibitor of DNA binding (*ID2*) and Krüppel-like factors 4 and 5 (*KLF4* and *KLF5*) were downregulated. Besides others, genes that were over-expressed only in cell lines with *N-RAS* mutations included glutathione *S*-transferase M1 and M4 (*GSTM1* and *GSTM4*), Ras-related GTP binding D (*RRAGD*) and dual specificity phosphatase 4 (*DUSP4*). Matrix metalloproteinase 14 (*MMP14*) and *FYN* oncogene were among the genes observed to be upregulated specifically in cell lines harbouring mutation in the *B-RAF* gene in comparison to cell lines without mutations.

Quantitative real-time PCR: validation of micro-array data

For a selected group of genes real-time PCR was used to validate the micro-array expression data. For this purpose we selected four genes with increased expression in cell lines with *B-RAF* and *N-RAS* mutations compared to cell lines without mutations and one gene that was upregulated only in cell lines with the *B-RAF* mutation. In addition we chose three genes under-expressed in cell lines with the *B-RAF* and *N-RAS* mutations and one gene downregulated only in cell lines with the *B-RAF* mutation in comparison with cell lines without mutations. The criterion for gene inclusion in real-time PCR experiments was its potential role in melanocyte biology, the MAPK pathway or cell cycle regulation.

Our results from real-time PCR confirmed micro-array data for all the selected genes. In micro-array experiments *DUSP6* showed an 8-fold over-expression in cell lines with mutations in the *B-RAF* and *N-RAS* genes relative to the cell lines without mutations and in real-time PCR experiments in a similar comparison isoform 'a' of *DUSP6* showed a 12-fold over-expression (Figure 4A); isoform 'b' showed only 2-fold upregulation (data not shown). The over-expression of *TAZ*, *SPRY2* and *AKT3* observed in micro-array experiments in cell lines with the mutations compared to cell lines without mutations were confirmed by RT–PCR (Figure 4B–D). The expression results from real-time PCR for *MMP14* were in agreement with micro-array data, which showed 4.5- and

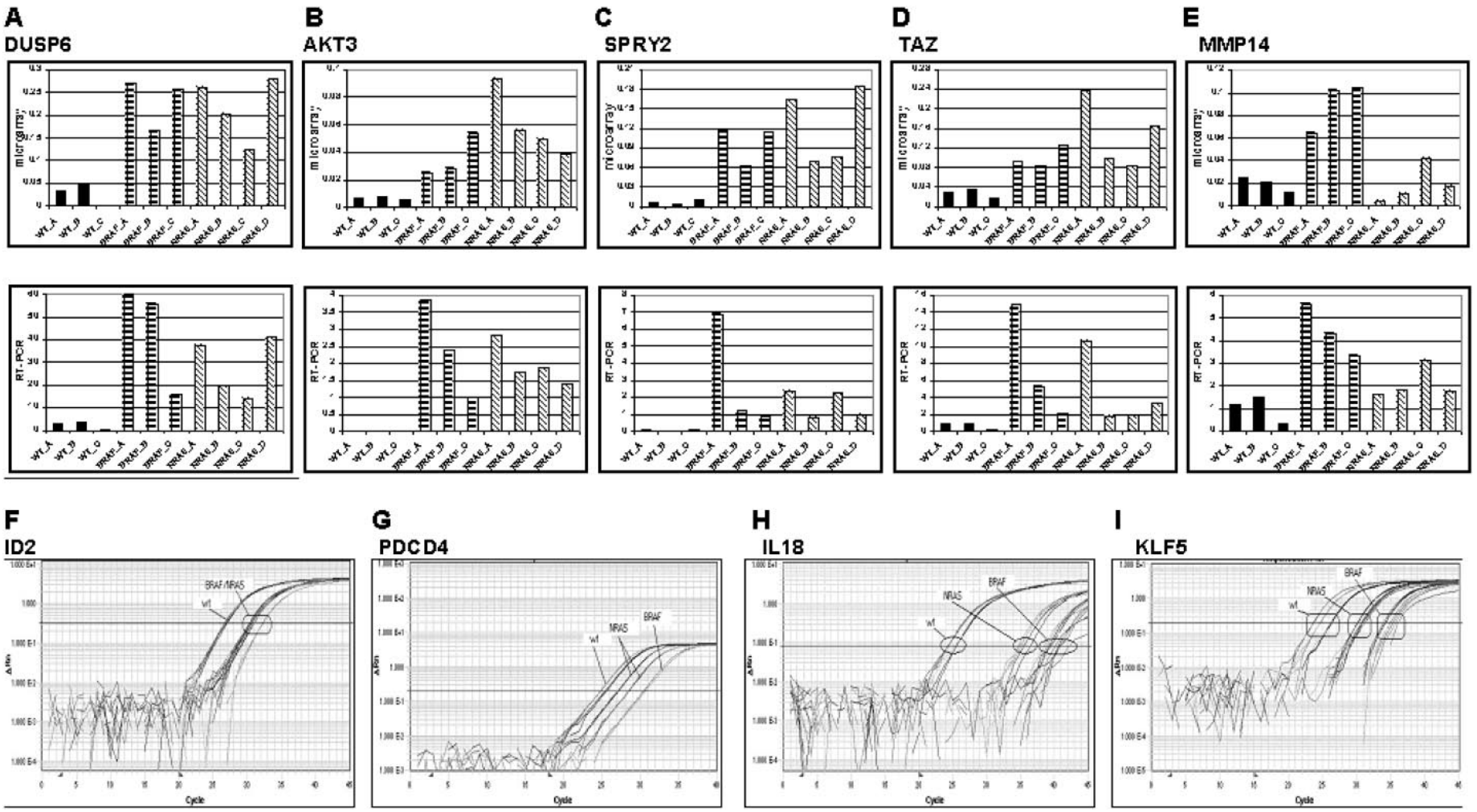

Fig. 4. The results from micro-array experiments for selected genes were validated with real-time PCR technique. (**A–E**) Panels show level of upregulation of genes from micro-array data (upper panels) and from RT–PCR data (lower panels). WT_A-C represent three cell lines without mutations; BRAF_A-C three cell lines with V600E mutation in the *B-RAF* gene and NRAS_A-D four cell lines with Q61R mutation in the *N-RAS* gene. The *y*-axis in upper panel in A–E represents micro-array signals normalized to β-actin and in lower panel *y*-axis represents real-time PCR signal intensity normalized to β-actin. (**F–I**) Panels show real-time amplification plots of four genes that were down-regulated in micro-array experiments in cell lines with mutations in the *B-RAF* and *N-RAS* genes compared to cell lines without mutations. See online supplementary material for a colour version of this figure.

4.6-fold increase, respectively, in cell lines with mutation in the *B-RAF* gene compared to cell without mutations (Figure 4E). However, in real-time experiments *MMP14* was also shown to be slightly over-expressed in cell lines with the *N-RAS* mutation (Figure 4E). The micro-array data for *TAZ* and *SPRY2* genes showed over-expression only in cell-lines with the *B-RAF* mutations (Supplementary Table I); however, in the real-time experiments both genes were confirmed as upregulated in all cell lines with the *B-RAF* or *N-RAS* mutation compared to cell lines with no mutations. In micro-array data analysis the filter was set for inclusion of probe sets with a signal log ratio of 1, which being 0.99 for *TAZ* and *SPRY2* genes in cell lines with *N-RAS* mutations resulted in their exclusion from the list of over-expressed genes.

Similarly, under-expression of *ID2* seen in micro-array experiments (4.8-fold) was confirmed for all cell lines harbouring mutations in the *B-RAF* and *N-RAS* genes versus cell lines without mutation in real-time PCR experiments (4.6-fold, Figure 4F). *PDCD4* was confirmed to be more drastically downregulated in cell lines with the mutant *B-RAF* (micro-array 5.3-fold/real time-PCR 5.7-fold) than in cell lines harbouring the *N-RAS* mutation (micro-array 1.7-fold/real-time PCR 1.9-fold, Figure 4G) when compared overall to the cell lines without mutations. *IL18* and *KLF5* expression was totally repressed in cell lines with mutations compared to the cell lines with no mutation (Figure 4H and I).

Discussion

In this study, we investigated the global gene expression profile of melanoma cell lines with the most potent and common mutation V600E in the *B-RAF* gene and compared it with the expression profile of melanoma cell lines with the common Q61R mutation in the *N-RAS* gene and with cell lines without mutations. Our results from the stringent analysis of the expression data, partly validated by quantitative real-time PCR showed (i) upregulation and downregulation of a number of genes with diverse and disparate molecular functions in cell lines with *B-RAF* and *N-RAS* mutations against cell lines without mutations; (ii) overlapping sets of over- and under-expressed genes in cell lines with *B-RAF* and *N-RAS* mutations; and (iii) distinct sets of up- or down-regulated genes that distinguish the cell lines with *B-RAF* and *N-RAS* mutations. Many of the genes with affected expression in melanoma cell lines due to mutations in the *B-RAF* and *N-RAS* genes encode constituents or regulators of the RAS/RAF/MEK/ERK and related pathways or are associated with metastasis or tumour invasiveness.

The group of genes prominently upregulated in melanoma cell lines with mutant *B-RAF* and *N-RAS* with a potential role direct or indirect, in the MAP-kinase pathways included a dual specificity phosphatase gene, *DUSP6*; an inhibitor of MAP-kinase signalling, *SPRY2*; a 14-3-3 binding protein encoding gene, *TAZ*; and oncogenic *AKT3* (19–22). *DUSP6* with a presumptive growth suppressor role causes both induction and inactivation of ERK1/2 through a potential feedback loop mechanism that involves non-catalytic binding (23). The localization of *DUSP6* in cytoplasm has been reported to effectively prevent translocation of ERK to target effectors inside the nucleus (19). The over-expression of *DUSP6* can be speculated to have a potential analogous role in the rescue of hyper-phosphorylated 'inactive' *B-RAF* (through a feed back loop), though, the putative phosphorylating sites in *B-RAF* similar to those discovered in *C-RAF* are not known (24).

Further, in concordance with an earlier report, we not only found relative over-expression of *SPRY2*, an inhibitor of MAP-kinase signalling in cell lines with *B-RAF* mutation, but also in cell lines with mutant *N-RAS*, albeit at a lower level than in cell lines with mutant *B-RAF* (25,26). In cell lines with mutations we also found relative over-expression of *AKT3*, which has been specifically shown to be deregulated at a high frequency in sporadic melanoma through an increased gene copy number and decreased PTEN expression (22). Interestingly, *B-RAF* contains several AKT phosphorylation sites and mutations affecting those residues have been reported in lung cancer (27). The inhibitory nature of AKT mediated phosphorylation of *B-RAF* together with over-expression observed in melanoma cells with mutant *B-RAF* and *N-RAS* highlight the complexities of cellular regulation or deregulation.

Some of the genes with distinct over-expression only in cell lines containing the *B-RAF* mutation included the *FYN* oncogene, genes belonging to melanoma antigen family, mitochondrial folate transporter and *MMP14* (28,29), whereas *GSTM4* and *RRAGD* were the genes upregulated specifically in cell lines with the *N-RAS* mutation compared to cell lines without mutations. Other over-expressed transcripts specific for cell lines with the *N-RAS* mutations included *ets* gene variants, which belong to a family of oncogenic transcription factors, several G-coupled protein receptors and *DUSP4* (23,30).

In cell lines with *B-RAF* and *N-RAS* mutations we found lack of *IL-18* cytokine expression, which is identified as a strong inducer of interferon-γ and its constitutive production can lead to an enhanced anti-tumour response and improved survival (31). Other genes with significantly reduced expression in cell lines with *B-RAF* and *N-RAS* mutation included *CD24* antigen, *KLF4*, *KLF5* and ID2 (32–34). CD24, a small heavily glycosylated mucin-like glycosylphosphatidyl-inositol-linked cell surface protein is expressed in a wide variety of human malignancies and is associated with a potential to metastasize (34).

In summary, our results provide novel insight into the effect of mutations in the *BRAF* and *N-RAS* genes on global gene expression in melanoma and highlight the complexity of mechanisms involved in tumour initiation and maintenance. In melanoma cell lines, we have shown the effect of the V600E mutation in *B-RAF* and the Q61R mutation in *N-RAS* on the transcription of various genes, many of which are involved in RAS/RAF-signalling and related pathways. The extent to which these results can be reproduced *in situ* remains to be seen. Moreover, gene expression analysis alone cannot provide an overall integrative molecular understanding of the genesis of melanoma and, therefore, these results need to be evaluated through mechanistic studies.

Supplementary material

Supplementary material can be found at: http://www.carcin.oupjournals.org/.

Conflict of Interest Statement: None declared.

References

1. Satyamoorthy,K., Li,G., Gerrero,M.R., Brose,M.S., Volpe,P., Weber,B.L., Van Belle,P., Elder,D.E. and Herlyn,M. (2003) Constitutive mitogen-activated protein kinase activation in melanoma is mediated by both *BRAF* mutations and autocrine growth factor stimulation. *Cancer Res.*, **63**, 756–759.
2. Smalley,K.S. (2003) A pivotal role for ERK in the oncogenic behaviour of malignant melanoma? *Int. J. Cancer*, **104**, 527–532.
3. Busca,R., Abbe,P., Mantoux,F., Aberdam,E., Peyssonnaux,C., Eychene,A., Ortonne,J.P. and Ballotti,R. (2000) Ras mediates the cAMP-dependent activation of extracellular signal-regulated kinases (ERKs) in melanocytes. *EMBO J.*, **19**, 2900–2910.
4. Halaban,R. (2000) The regulation of normal melanocyte proliferation. *Pigment Cell Res*, **13**, 4–14.
5. Davies,H., Bignell,G.R., Cox,C. *et al.* (2002) Mutations of the *BRAF* gene in human cancer. *Nature*, **417**, 949–954.
6. Kumar,R., Angelini,S., Czene,K., Sauroja,I., Hahka-Kemppinen,M., Pyrhonen,S. and Hemminki,K. (2003) BRAF mutations in metastatic melanoma: a possible association with clinical outcome. *Clin. Cancer Res.*, **9**, 3362–3368.
7. Kumar,R., Angelini,S. and Hemminki,K. (2003) Activating *BRAF* and *N-Ras* mutations in sporadic primary melanomas: an inverse association with allelic loss on chromosome 9. *Oncogene*, **22**, 9217–9224.
8. Kumar,R., Angelini,S., Snellman,E. and Hemminki,K. (2004) *BRAF* mutations are common somatic events in melanocytic nevi. *J. Invest. Dermatol.*, **122**, 342–348.
9. Pollock,P.M., Harper,U.L., Hansen,K.S. *et al.* (2003) High frequency of *BRAF* mutations in nevi. *Nat. Genet.*, **33**, 19–20.
10. Wan,P.T.C., Garnett,M.J., Roe,S.M. *et al.* (2004) Mechanism of activation of the RAF–ERK signaling pathway by oncogenic mutations of *B-RAF*. *Cell*, **116**, 855–867.
11. Wellbrock,C., Ogilvie,L., Hedley,D., Karasarides,M., Martin,J., Niculescu-Duvaz,D., Springer,C.J. and Marais,R. (2004) *V599EB-RAF* is an oncogene in melanocytes. *Cancer Res.*, **64**, 2338–2342.
12. Andersen,M.H., Fensterle,J. and Ugurel,S. (2004) Immunogenicity of constitutively active V599EBRaf. *Cancer Res.*, **64**, 5456–5460.
13. Hingorani,S.R., Jacobetz,M.A., Robertson,G.P., Herlyn,M. and Tuveson,D.A. (2003) Suppression of *BRAF*(V599E) in human melanoma abrogates transformation. *Cancer Res.*, **63**, 5198–5202.
14. Rotolo,S., Diotti,R., Gordon,R.E., Qiao,R.F., Yao,Z., Phelps,R.G. and Dong,J. (2005) Effects on proliferation and melanogenesis by inhibition of mutant *BRAF* and expression of wild-type *INK4A* in melanoma cells. *Int. J. Cancer*, **115**, 164–169.
15. Omholt,K., Karsberg,S., Platz,A., Kanter,L., Ringborg,U. and Hansson,J. (2002) Screening of N-ras codon 61 mutations in paired primary and metastatic cutaneous melanomas: mutations occur early and persist throughout tumor progression. *Clin. Cancer Res.*, **8**, 3468–3474.
16. Pavey,S., Johansson,P., Packer,L. *et al.* (2004) Microarray expression profiling in melanoma reveals a *BRAF* mutation signature. *Oncogene*, **23**, 4060–4067.
17. Tusher,V.G., Tibshirani,R. and Chu,G. (2001) Significance analysis of microarrays applied to the ionizing radiation response. *Proc. Natl Acad. Sci. USA*, **98**, 5116–5121.
18. Tamayo,P., Slonim,D., Mesirov,J., Zhu,Q., Kitareewan,S., Dmitrovsky,E., Lander,E.S. and Golub,T.R. (1999) Interpreting patterns of gene expression with self-organizing maps: methods and application to hematopoietic differentiation. *Proc. Natl Acad. Sci. USA*, **96**, 2907–2912.
19. Furukawa,T., Sunamura,M., Motoi,F., Matsuno,S. and Horii,A. (2003) Potential tumor suppressive pathway involving DUSP6/MKP-3 in pancreatic cancer. *Am. J. Pathol.*, **162**, 1807–1815.
20. Hanafusa,H., Torii,S., Yasunaga,T. and Nishida,E. (2002) Sprouty1 and Sprouty2 provide a control mechanism for the Ras/MAPK signalling pathway. *Nat. Cell Biol.*, **4**, 850–858.
21. Kanai,F., Marignani,P.A., Sarbassova,D. *et al.* (2000) TAZ: a novel transcriptional co-activator regulated by interactions with 14-3-3 and PDZ domain proteins. *EMBO J.*, **19**, 6778–6791.
22. Stahl,J.M., Sharma,A., Cheung,M., Zimmerman,M., Cheng,J.Q., Bosenberg,M.W., Kester,M., Sandirasegarane,L. and Robertson,G.P. (2004) Deregulated Akt3 activity promotes development of malignant melanoma. *Cancer Res.*, **64**, 7002–7010.
23. Theodosiou,A. and Ashworth,A. (2002) MAP kinase phosphatases. *Genome Biol.*, **3**, REVIEWS3009.
24. Dougherty,M.K., Muller,J., Ritt,D.A., Zhou,M., Zhou,X.Z., Copeland,T.D., Conrads,T.P., Veenstra,T.D., Lu,K.P. and Morrison,D.K. (2005) Regulation of raf-1 by direct feedback phosphorylation. *Mol. Cell*, **17**, 215–224.
25. Tsavachidou,D., Coleman,M.L., Athanasiadis,G., Li,S., Licht,J.D., Olson,M.F. and Weber,B.L. (2004) SPRY2 is an inhibitor of the ras/extracellular signal-regulated kinase pathway in melanocytes and melanoma cells with wild-type BRAF but not with the V599E mutant. *Cancer Res.*, **64**, 5556–5559.
26. Yusoff,P., Lao,D.H., Ong,S.H., Wong,E.S., Lim,J., Lo,T.L., Leong,H.F., Fong,C.W. and Guy,G.R. (2002) Sprouty2 inhibits the Ras/MAP kinase pathway by inhibiting the activation of Raf. *J. Biol. Chem.*, **277**, 3195–3201.
27. Brose,M.S., Volpe,P., Feldman,M. (2002) *BRAF* and *RAS* mutations in human lung cancer and melanoma. *Cancer Res.*, **62**, 6997–7000.
28. Palacios,E.H. and Weiss,A. (2004) Function of the Src-family kinases, Lck and Fyn, in T-cell development and activation. *Oncogene*, **23**, 7990–8000.
29. Iida,J., Wilhelmson,K.L., Price,M.A., Wilson,C.M., Pei,D., Furcht,L.T. and McCarthy,J.B. (2004) Membrane type-1 matrix metalloproteinase promotes human melanoma invasion and growth. *J. Invest. Dermatol.*, **122**, 167–176.
30. Oikawa,T. (2004) ETS transcription factors: possible targets for cancer therapy. *Cancer Sci.*, **95**, 626–633.
31. Nagai,H., Hara,I., Horikawa,T., Oka,M., Kamidono,S. and Ichihashi,M. (2002) Gene transfer of secreted-type modified interleukin-18 gene to B16F10 melanoma cells suppresses *in vivo* tumor growth through inhibition of tumor vessel formation. *J. Invest. Dermatol.*, **119**, 541–548.
32. Bieker,J.J. (2001) Kruppel-like factors: three fingers in many pies. *J. Biol. Chem.*, **276**, 34355–34358.
33. Russell,R.G., Lasorella,A., Dettin,L.E. and Iavarone,A. (2004) Id2 drives differentiation and suppresses tumor formation in the intestinal epithelium. *Cancer Res.*, **64**, 7220–7225.
34. Kristiansen,G., Sammar,M. and Altevogt,P. (2004) Tumour biological aspects of CD24, a mucin-like adhesion molecule. *J. Mol. Histol.*, **35**, 255–262.

Received December 6, 2004; revised January 28, 2005; accepted February 26, 2005